Biogeochemistry **59:** 207–237, 2002.

Application of a transport-reaction model to the estimation of biogas fluxes in the Scheldt estuary

J.P. VANDERBORGHT[1], R. WOLLAST[1], M. LOIJENS[1] & P. REGNIER[2]
[1]*Université Libre de Bruxelles Laboratory of Chemical Oceanography Bd du Triomphe, CP 208, B-1050 Brussels, Belgium;* [2]*Utrecht University Department of Geochemistry P.O. Box 80021, NL-3508 TA Utrecht, The Netherlands*

Received 3 July 2000

Key words: biogas fluxes, CO_2, estuary, N_2O, Scheldt, transport-reaction model

Abstract. In the frame of the BIOGEST project, the full transient, one-dimensional, reactive-transport model CONTRASTE has been extended for the computation of biogases in the Scheldt estuary. The CONTRASTE model (**Co**upled, **N**etworked, **T**ransport-**R**eaction **A**lgorithm for **S**trong **T**idal **E**stuaries) provides a satisfactory description of the estuarine residual circulation (including daily freshwater discharge and a complete description of the tide) and a flexible implementation of the various physico-chemical and biological transformations, including both kinetically-controlled and equilibrium reactions. The model allows resolution of the complex, nonlinear collective behaviour of this type of system and investigation of the non-steady-state phenomena which govern estuarine dynamics. Variables currently implemented in the model include salinity, suspended matter, oxygen, inorganic carbon species, degradable organic carbon and nitrogen, inorganic nitrogen species, freshwater and marine phytoplankton. Biological processes described are heterotrophic respiration, primary production, nitrification and denitrification. Equilibrium formulations allow for DIC and NH_4^+/NH_3 speciation. Physical processes include gas transfer at the water/air interface, depending on both wind speed and current velocity. pH profiles are explicitly computed and constitute a very sensitive check of the overall model consistency. Results of the CONTRASTE model are in very good agreement with the measured longitudinal distribution of the variables considered, in particular O_2, pH, pCO_2 and N_2O concentrations. However, discrepancies are observed between the calculated fluxes of CO_2 and those estimated using an *in situ* floating chamber. It is shown that the evaluation of gas transfer can be affected by serious errors if the variations due to changes in current velocity and water depth during one tidal cycle are not taken into consideration. The model also shows that the fluxes of biogases in estuaries are greatly influenced by the quasi-exponential increase of the exchange surface area with decreasing distance to the sea. Our estimation of the total daily flux of O_2, CO_2 and N_2O is equal to +28500, –19000 and –17 kmoles.day^{-1} respectively for the Scheldt estuary in July 1996.

Introduction

Estuaries are highly dynamic systems characterised by large chemical and biological gradients which render flux estimations difficult. This is particu-

larly true for tidal estuaries such as those investigated during the BIOGEST project, which have their dynamics dominated by tidal forcing and where the residence time of fresh water in the mixing zone is fairly long. This permits significant transformations of material carried by fresh water. Flux estimations in strong tidal estuaries are further complicated by the fact that steady-state is rarely approached in these systems because of the fluctuating boundary conditions and nonlinearities of the fluid motion. Strong variations in river inflow and in the composition of fresh water input require a detailed knowledge of the upstream boundary conditions. All these fluctuations generate important storage or depletion terms for constituents within the estuary (Regnier et al. 1998). In order to estimate the fluxes of constituents in tidal estuaries, a full transient multicomponent reactive transport model (CONTRASTE) was developed and applied to the Scheldt (Regnier et al. 1997, 1998; Regnier & Steefel 1999). This model provides a satisfactory description of the estuarine residual circulation, taking into account daily runoff values and forcing from tidal oscillations. It includes biogeochemical interactions through the description of kinetically mediated processes and simultaneous equilibrium reactions. Our task in the BIOGEST project was to extend this model to the calculation of the fluxes of biogases in the Scheldt estuary in order to provide a tool allowing correct estimations of atmospheric fluxes, over a large spectrum of time scales.

The Scheldt is located in a heavily populated area where intensive agricultural and industrial activities occur. This estuary is therefore strongly disturbed by the anthropogenic activities (Wollast 1988). The high organic carbon load entering the estuary is due not only to the discharge of untreated wastewater but also to the large photosynthetic primary production observed in the highly eutrophicated riverine system. In the upper estuary, pCO_2 values exceed systematically 5000 μatm and are responsible for large fluxes of this gas to the atmosphere (Frankignoulle et al. 1996, 1998). It is also characterised by intensive nitrification which is responsible for strong oversaturation of N_2O (De Wilde & De Bie 2000). The longitudinal profile of dissolved N_2O indicates that this component is lost to the atmosphere within the estuary rather than being transported to the open sea. Furthermore, the nitrification process results in the acidification of the estuarine waters and enhances the pCO_2 values, favouring the CO_2 transfer to the atmosphere (Frankignoulle et al. 1996). The CONTRASTE model was thus extended to quantify the various biological and chemical processes responsible for the production of these two greenhouse gases and to estimate their fluxes at the water-air interface. The simulation presented here corresponds to a two-month period of high biological activity (June–July) characterized by extreme atmospheric fluxes of both CO_2 and N_2O. Furthermore, during this period, it was possible to

compare the predictions of the model with a comprehensive set of BIOGEST field data collected in the Scheldt estuary between the 8th and the 12th of July 1996.

The CONTRASTE model

The mathematical formulation of the CONTRASTE model is described in detail in Regnier et al. (1997) and in Regnier and Steefel (1999). This model combines a one-dimensional hydrodynamic description with a set of algorithms for advective and dispersive solute transport, and mixed multi-component reactions. The 1-D hydrodynamical model provides the water elevation, the estuarine width, the instantaneous flow and the cross-sectional average velocity at each grid point and for each time step. The coupled transport-reaction model evaluates concentrations and rates at the same grid points, as well as fluxes through any cell interface, including the water- atmosphere boundary layer. The time resolution of the model (150 s) is sufficiently high to include the short-term components of the tide. This is especially important for the computation of the gas-transfer rates, which depend highly on the changes in water depth and current velocity. The hydrodynamical model covers the entire length of the Scheldt influenced by the tide, extending up to 150 km from the estuarine mouth.

The integrated forms of continuity and momentum equations for a channel with arbitrary geometry are given by (Regnier et al. 1998):

$$\frac{\partial A}{\partial t} = -\frac{\partial Q}{\partial x} \tag{1}$$

$$\underset{\text{local acc.}}{\frac{\partial Q}{\partial t}} + \underset{\text{convective acc.}}{\frac{\partial}{\partial x}\left(\frac{QQ}{A}\right)} + \underset{\text{pressure grad.}}{Ag\frac{\partial \xi}{\partial x}} + \underset{\text{friction}}{k\frac{Q^2 L}{A^2}} = 0 \tag{2}$$

where:

t	time, [s]
x	distance along the river axis, [m]
A(x, t)	cross-section, [m^2]
Q(x, t)	instantaneous flow, [$m^3.s^{-1}$]
g	gravitational acceleration, [$m.s^{-2}$]
ξ(x, t)	elevation, [m]
k	dimensionless friction coefficient
L(x, t)	estuarine width, [m].

The governing nonlinear partial differential equations are solved using a finite difference scheme, with a spatial discretization of 2 km. The resulting 116 grid points include all the major tributaries, while the continuity equation takes into account the irregular variations of the estuarine width. The boundary conditions that must be provided to the hydrodynamic model are the water elevation at the estuarine mouth and the river discharge at the upstream nodes. The first condition (open-sea tidal forcing) is computed from a sum of harmonics (Dronkers 1964), while the second condition is extracted from a database of daily mean water discharge of the Scheldt river and its tributaries. As model tests have shown, the output becomes independent of the initial conditions when the simulation is started at least one month before the period of interest. In this case, the initial conditions can be arbitrarily selected.

The coupling of mass transport and chemical reactions can be described by a set of partial differential equations of the form:

$$\frac{\partial(AC_j)}{\partial t} + \frac{\partial(QC_j)}{\partial x} = \frac{\partial}{\partial x}\left(AK\frac{\partial C_j}{\partial x}\right) + AR_j \ (j = 1 \ldots N_{tot}) \qquad (3)$$

where:

C_j	concentration of the species j, [kg.m^{-3}]
K	dispersion coefficient, [m^2.s^{-1}]
R_j	process rate affecting species j, [kg.m^{-3}.s^{-1}]

The reaction term R_j may include both kinetically-controlled biogeochemical reactions, kinetic gas exchange and fast (equilibrium) reactions. The reactive-transport model presented here is restricted to the mixing zone situated between Vlissingen (km 0) and a point situated below the confluence of the Rupel river (km 90). Concentrations and fluxes are computed by the model for the corresponding 45 cells.

Species currently implemented in the model are listed in Table 1. In addition to advective and diffusive transport mechanisms, these various species are subjected to a number of physical, chemical and biological processes which are summarized in Figure 1 and briefly described in the following paragraphs. A detailed presentation of the processes and reactions currently implemented in CONTRASTE can be found at the web site devoted to the model: *http://www.geo.uu.nl/Research/Geochemistry/kb*.

In this model application, the mass transfer through the sediment – water interface has not been taken into consideration. Indeed, it has been demonstrated that at the estuarine scale, these exchanges represent only a small fraction of the overall budgets (Regnier & Steefel 1999). The main reasons for this could be attributed to (1) the low value of the estuarine surface to volume

Table 1. State variables explicitly considered in the model

Salinity
pH
Dissolved O_2
Suspended particulate matter
Dissolved inorganic carbon:
CO_2
H_2CO_3
HCO_3^-
CO_3^{2-}
Labile dissolved organic carbon
Dissolved inorganic nitrogen:
NH_4^+
NO_2^-
NO_3^-
N_2O
Labile dissolved organic nitrogen
Freshwater phytoplankton
Marine phytoplankton
Biomass of nitrifying bacteria

ratio; (2) the mixing, resuspension and deposition of the upper part of the bottom layer during the tidal cycle. As a consequence, the biological activity associated with the sediment is actually taking place in the water column for a part of the time.

Gas transfer at the air/water interface is of concern for the four biogases O_2, CO_2, N_2O and NH_3. The rate of the transfer process is classically expressed by the product of a piston velocity by a concentration gradient at the interface, with the piston velocity of oxygen taken as a reference. It is expressed as the sum of two terms, respectively linked to the wind speed and to the current velocity. Wind speed contribution to the overall transfer is a function of u_{10}^2 (u_{10} being the wind speed at 10 m height) and of the Schmidt number, according to the expression of Wanninkhoff (1992). The Schmidt number (a function of both the molecular diffusion coefficient of O_2 and of the viscosity of water) is in turn dependent on temperature and salinity of the water column. The contribution of the current velocity is described by the classical formulation of O'Connor and Dobbins (1956), i.e. a dependence on the square root of the velocity to depth ratio. For other biogases, piston velocities are computed using their molecular diffusion ratios with respect to

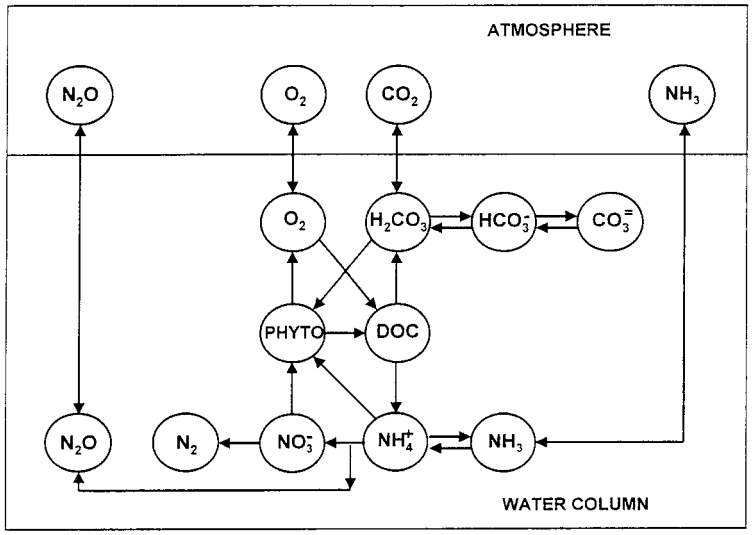

Figure 1. Biological and chemical processes affecting the species described in the CONTRASTE model.

oxygen. Concentration gradients at the interface are expressed as the difference between the bulk water concentration and the equilibrium concentration with respect to the atmosphere. The following references have been used to compute the value of the equilibrium concentration of the considered biogases as a function of temperature and salinity: Benson and Krause (1984) for O_2, Weiss and Price (1980) for CO_2 and N_2O, Sander (1999) for NH_3.

The main chemical processes included in the model are the equilibrium reactions between (1) dissolved inorganic carbon species and (2) ammonium and ammonia. For dissolved inorganic carbon (DIC) species, the apparent dissociation constant K_1' and K_2' are precisely known for fresh water and seawater, but our knowledge is more limited when large variations of salinity are involved, as in the case of estuarine environments. We have selected here the temperature-salinity dependency proposed by Cai and Wang (1998). According to these authors, deviations from Mook and Koene (1975) or from Edmund and Gieskes (1970) at low salinity, and from Mehrbach et al. (1973) at high salinity, for the whole temperature (0.2–35 °C) and salinity (0–40) ranges, are $< \pm 0.015$ for pK_1' and $< \pm 0.04$ for pK_2'. The apparent dissociation constant for ammonia is computed from the expression of Clegg and Whitfield (1995).

Biological processes described in the model are heterotrophic respiration, primary production, nitrification (including nitrogen oxide production) and denitrification. Aerobic degradation by heterotrophic organisms, excluding higher trophic levels, is described by a classical Michaelis-Menten (M-M)

kinetic with a dependency on both organic matter and oxygen concentrations. The rate of denitrification is also expressed by an M-M type formulation depending on nitrate and organic substrate concentrations, and an inhibition term for oxygen is included in the rate law. The primary production module allows for the computation of gross primary production (GPP), respiration and cell decay for two types of phytoplanktonic populations, respectively of fresh water and marine origin. In the nutrient-enriched Scheldt estuary, the photosynthetic activity is mainly controlled by light availability, and the model evaluation of GPP is based on the classical hyperbolic response of the photosynthetic activity P with respect to the light intensity I (Platt et al. 1980). The P-I curve is characterized by two parameters: the photosynthetic efficiency α and the optimal light intensity I_k (which is equal to the maximum rate of photosynthesis P_{max} at saturating light intensity divided by α). Because of light limitation in the Scheldt estuary, no nutrient- and light-inhibition factors are considered in the model (although ammonia or nitrate uptake through the process of algal growth is taken into account). The surface irradiance, which is a function of the time of the day, is parameterized according to Platt et al. (1990). It also depends on the percentage of cloud coverage, which is taken from meteorological records for the period considered (IRM 1996). From the value of the local extinction coefficient, an exponentially decreasing vertical profile of photosynthetically active radiation (PAR) in the water column is calculated for each grid point of the model, and a depth-averaged GPP is obtained by integration. Note that the value of the extinction coefficient is computed from a simple linear relationship with respect to the suspended matter concentration. For primary production estimation, the longitudinal variation of turbidity is modelled according to the formulation proposed by Soetaert and Herman (1993). This formulation relates the amount of suspended matter to the position along the estuary and to the freshwater discharge only.

To estimate the net primary production (NPP), the autotrophic algal respiration must be subtracted from the computed GPP. This respiration term is the sum of two contributions associated with biosynthesis and maintenance. The former is assumed to be proportional to the GPP, while the latter is a linear function of the phytoplankton pool. Finally, the model includes a cell decay term, which combines cell lysis and grazing by higher trophic levels into a single first-order rate expression. In addition, a salinity stress function is incorporated into the growth rate equations to express the adaptation of both fresh water and seawater phytoplankton to the salinity conditions (Billen et al. 1988).

The two steps involved in the nitrification process (ammonia oxidation to nitrite and nitrite oxidation to nitrate) are considered in the model. The

M-M rate law for each step includes a dependency towards oxygen and the relevant nitrogenous species (NH_4^+ and NO_2^- respectively). The biomass of nitrifying bacteria is explicitly considered in the rate expressions. Nitrogen oxide production is considered as only due to nitrification, and the rate of N_2O formation is computed using a constant yield (mole of N_2O produced per mole of NH_4^+ oxidized). For all biological processes involved, a temperature function (and for nitrification, a pH function; Brion & Billen 1998) is incorporated into the kinetic expressions.

Evolution of the parameters along a longitudinal profile during the July 1996 cruise

During the BIOGEST cruise conducted in July 1996 on board of the RV Belgica, numerous physical, chemical and biological parameters were measured in the mixing zone of the Scheldt. The complete set of field data from this cruise is available on the BIOGEST web site at: *http://www.ulg.ac.be/oceanbio/biogest/biogest.htm*. We present here briefly the most relevant ones for our purpose (Figure 2). They confirm the general trends described in previous investigations (Somville 1984; Wollast 1988; Frankignoulle 1996) and the continuous improvement of the water quality in the estuary, as a result of the gradual implementation of wastewater treatment plants (Van Damme et al. 1995).

The longitudinal profile of oxygen clearly demonstrates the occurrence of sub-oxic conditions in the upper estuary due not only to the respiration of detrital organic matter but also to the nitrification process which concomitantly removes large quantities of ammonia and increases the NO_2^-/NO_3^- concentrations. Respiration of dissolved organic carbon affects only slightly the distribution of DOC, which behaves almost like a conservative parameter. The values of DOC reported here are those measured by catalytic oxidation at high temperature. However, most of this large organic load is very refractory to bacterial degradation: long-term measurements of oxygen consumption for summer conditions indicate that only 10% of the organic matter is respired after one month. The consumption of oxygen in the upper estuary is not compensated by the photosynthetic activity occurring in this area. In fact, the high concentrations of phytoplankton observed upstream reflects the intensive photosynthetic activity taking place in the upper catchment of the river basin. Our measurements of the specific photosynthetic parameters of the phytoplankton populations indicate that the organisms are rapidly decaying when the salinity increases, and this process probably contributes to the production of easily degradable organic matter.

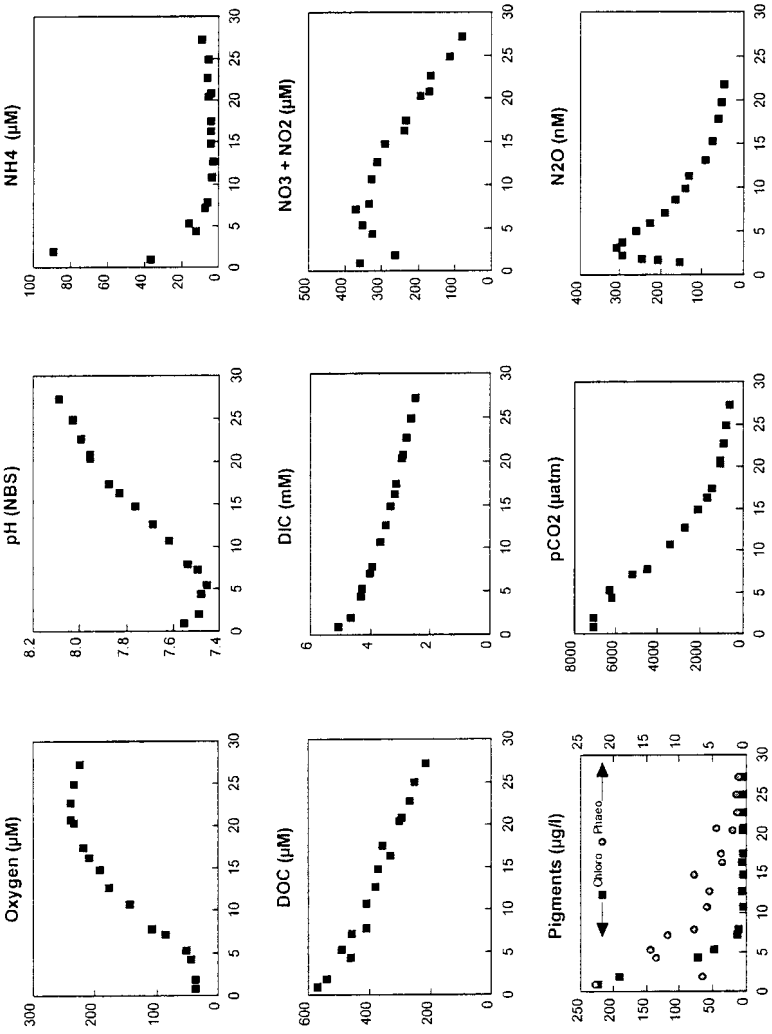

Figure 2. Longitudinal concentration profiles measured during the July 1996 BIOGEST cruise (database: web site http://www.ulg.ac.be/oceanbio/biogest/biogest.htm and N_2O profile from de Wilde and de Bie (2000)).

Respiration and especially nitrification is responsible for the pH drop observed in the upper estuary. This acidification increases drastically the partial pressure of CO_2 which remains oversaturated with respect to the atmosphere all over the estuary. The small deviation from the conservative behaviour of inorganic carbon may be attributed to the degassing of CO_2 which is very important upstream (Frankignoulle et al. 1996). Nitrification is also responsible for the high concentrations of N_2O reported by De Wilde and De Bie (2000).

Boundary conditions of the model

The boundary conditions that must be provided to run the hydrodynamic model are the water elevation at the estuarine mouth and the upstream fresh water discharge of the Scheldt and its tributaries. The tidal amplitude at the mouth varies between 2.1 and 5.2 meters with a mean value of 3.5 m. The river flow over one year (Figure 3) is characterised by extremely high variability. Fast transient fluctuations of the river discharge on the order of a few days are superimposed onto the seasonal evolution, resulting in far from steady-state conditions for the constituents within the estuarine domain (Regnier et al. 1997). However, during the June–July 1996 period, the river discharge remained rather stable and low, at around 35 $m^3.s^{-1}$. In order to obtain the boundary conditions for the biogeochemical variables involved in the model, weekly measurements of a number of chemical parameters were performed over the year at a fixed station situated at the limit of the salt intrusion (km 90). The input parameters are conductivity, temperature, alkalinity, pH, dissolved oxygen, nitrate, nitrite, ammonia and chlorophyll. The most important variables are represented in Figure 3. It can be seen that the upper part of the estuary remains sub-oxic all over the year except during short events of high water discharge occurring during the winter. The evolution of the photosynthetic activity which exhibits a maximum during the summer is well demonstrated by the annual profile of chlorophyll. Figure 3 also shows that there are strong fluctuations in the concentrations of nitrate and ammonia in the river input to the estuary. The total dissolved inorganic nitrogen exhibits a strong maximum during the winter flood events due to agricultural land washout. The concentration of nitrate is very dependent on the rates of nitrification and denitrification which are in turn influenced by the concentration of oxygen in the river system. The alkalinity and pH are used to define the speciation of the dissolved inorganic species. The maximum alkalinity is observed in winter and can exceed 5 meq/l. The pH exhibits small fluctuations between 7.35 and 7.75. These small changes are however sufficient to induce strong fluctuations in pCO_2. For the period covered by

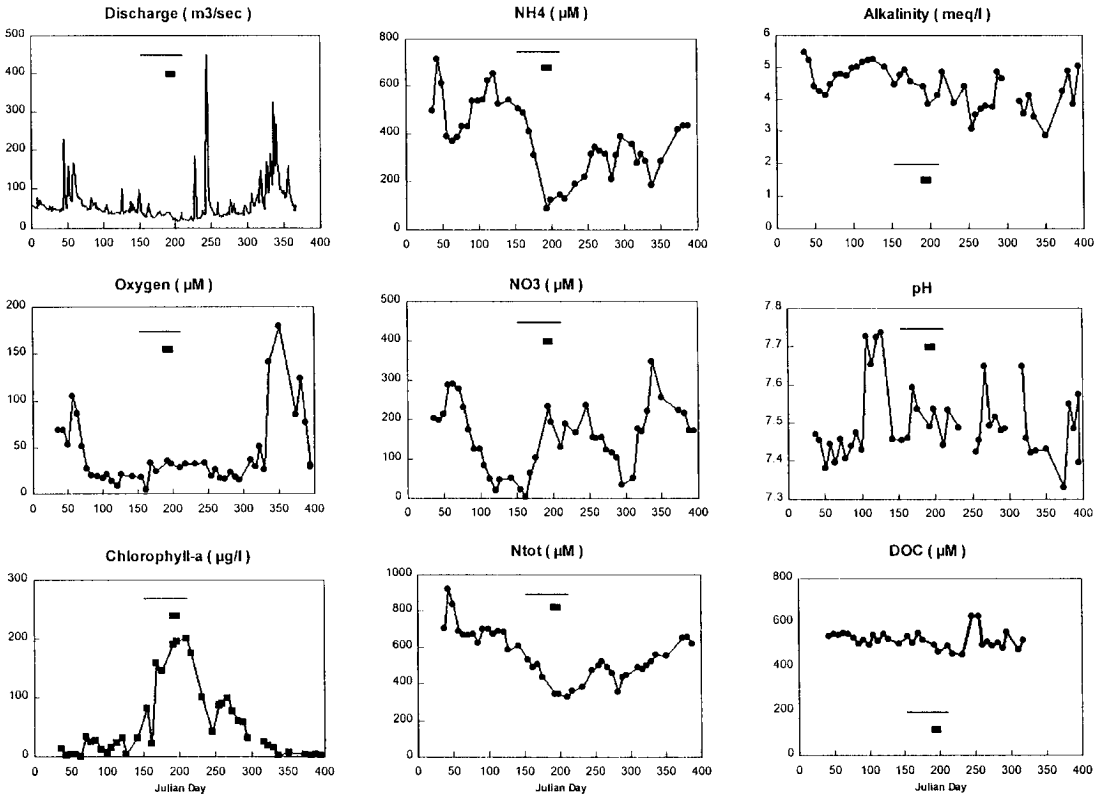

Figure 3. Annual upstream boundary conditions measured at Hemiksem (km 90 from the mouth). The horizontal thin line corresponds to the model run period and the thick line to the July 1996 BIOGEST cruise. (Discharge data provided by the Ministerie van de Vlaamse Gemeenshap, Department Leefmilieu en Infrastructuur, Afdeling Maritieme Schelde, Belgium).

Table 2. Boundary conditions at the mouth of the estuary for the run June–July 1996

Salinity	30.3	
O_2	227	μM
NO_3^-	36	μM
NO_2^-	2	μM
NH_4^+	10	μM
DOC total	176	μM
DOC labile	10	μM
Alkalinity	2.53	mequ/l
pH	8.20	NBS scale
chlorophyll	4	μg/l

the model run, the pCO_2 of the water entering the estuary was fluctuating around 5600 μatm, which represents an oversaturation with respect to the atmosphere exceeding 1500%. The input of organic carbon is less easy to quantify. The concentration of DOC, measured by catalytic oxidation at high temperature, remains rather constant over the year (around 470 μM). As indicated earlier, only a small fraction of this carbon ($\sim$10%) is sufficiently reactive to be respired in the estuary. We have therefore decided to fix the concentration of labile dissolved organic carbon at 47 μm. In addition to the river supply, point discharges are situated in the estuarine region including inputs from domestic, industrial and agricultural activities. These contributions were quantified on the basis of an extensive database (SAWES 1991). On a yearly basis, they represent 33% of the total N input and 49% of the total easily degradable organic carbon.

The boundary conditions at the mouth of the estuary are easier to define since they are rather stable over periods of time of one month, except during flood events. In addition, they exert in general a much weaker influence on the biogeochemistry of the estuarine domain. The values of the parameters, assumed constant during the period of the simulation, are based on the measurements performed during the July 96 BIOGEST cruise. They are given in Table 2.

Results

All model results reported below correspond to day 40 of the simulation run (10 July 1996). Field data were collected during the BIOGEST cruise (8th–

Table 3. Biogeochemical process rates. Values of the parameters for the June–July 1996 run. All rates are given at 10°C

Heterotrophic respiration:	
Maximum rate: 2.0×10^{-10} [M.s^{-1}]	
Half-saturation concentration for organic substrate: 6.0×10^{-5} [M C]	
Half-saturation concentration for oxygen : 1.5×10^{-5} [M O_2]	
Nitrification:	
Mortality of nitrifrifying biomass: 2.0×10^{-6} [s^{-1}1]	
Ammonia oxidation to nitrite:	
Maximum growth rate: 5.0×10^{-5} [s^{-1}]	
Half-saturation concentration for ammonium: 1.0×10^{-4} [M N]	
Half-saturation concentration for oxygen: 1.5×10^{-5} [M O_2]	
Yield: 9.0×10^{-2} (mole C synthesized per mole NH_4^+ consumed)	
Nitrite oxiodation to nitrate:	
Maximum growth rate: 2.0×10^{-5} [s^{-1}]	
Half-saturation concentration for nitrite: 2.0×10^{-6} [M N]	
Half-saturation concentration for oxygen: 3.0×10^{-5} [M O_2]	
Yield: 2.0×10^{-2} (mole C synthesized per mole NO_2^- consumed)	
N_2O production:	
Yield: 3.0×10^{-3} (mole N_2O produced per mole NH_4^+ oxidized)	
Denitrification:	
Maximum rate: 2.0×10^{-10} [M.s^{-1}]	
Half-saturation concentration for nitrate: 4.5×10^{-5} [M N]	
Half-saturation concentration for organic substrate: 6.0×10^{-5} [M C]	
Half-saturation concentration for oxygen inhibition: 2.0×10^{-5} [M O_2]	
Primary production:	
Maximum production: 4.7×10^{-5} [s^{-1}]	
Optimal light intensity I_k: 4.36×10^{-4} [E.m^{-2}.s^{-1}]	
Phytoplankton respiration rate – maintenance: 5.6×10^{-7} [s^{-1}]	
Phytoplankton respiration rate – biosynthesis: 3.2×10^{-1} [–]	
Phytoplankton mortality: 4.2×10^{-7} [s^{-1}]	

12th July 1996). The values of the various kinetic parameters used in the rate expressions are summarized in Table 3.

Hydrodynamic model

The hydrodynamic model allows for the description of the instantaneous exchanges of water at each grid point. In the summer period of 1996, the

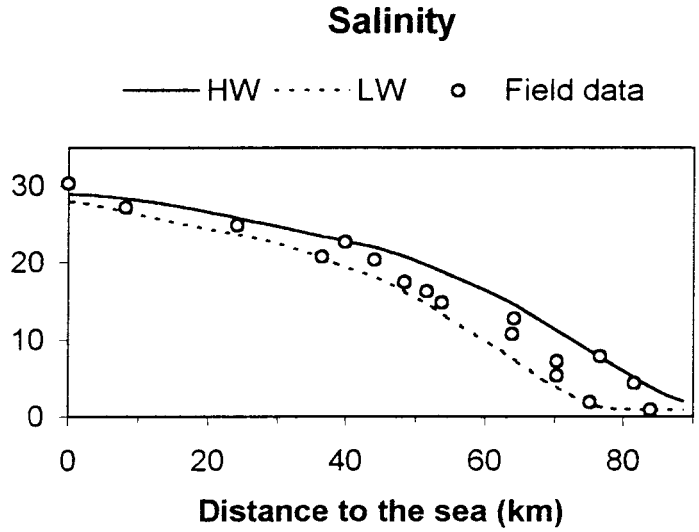

Figure 4. Salinity profiles calculated for high tide (HW) and low tide (LW) and compared to field data.

average volume of water flowing during one half tidal period was around 50×10^6 m^3 upstream and around 1000×10^6 m^3 at the mouth of the estuary. The computed residual flow at the outlet, which takes into account the spring-neap tidal cycle, is equal to 31 $m^3.s^{-1}$, which is close to the imposed fresh water input at the river end (35 $m^3.s^{-1}$). The calculations show that the volume of fresh water in the estuary remained fairly constant during this period. The validity of the 1-D solute transport model can be easily checked by comparing the observed salinities with the calculated profiles. Since the salinities were measured during one week at various periods of the tide, we have represented in Figure 4 the salinity profiles calculated at low and high tide for the period considered. This figure shows that all field data are well within the range predicted by the model. In the following discussion, salinity will be considered as the conservative variable, which will be used to characterize the water masses. Accordingly, all longitudinal profiles will be expressed as a function of salinity. This allows to avoid the short term fluctuations due to the tide, and, consequently, to circumvent the inherent difficulties associated with asynchronous measurements.

Organic matter

It is necessary to distinguish here between the refractory organic matter which is not affected by bacterial respiration during its transfer through the estuary, and the easily degradable fraction. Dilution is the only process controlling

the concentration of dissolved refractory organic carbon and the longitudinal profile is simply represented by a straight line in a concentration-salinity diagram, under the quasi-stationary conditions prevailing during the period considered. Both dissolved and particulate labile organic carbon is supplied to the estuary through upstream and lateral inputs. During the summer, nearly all the particulate organic matter is in the form of living or dead phytoplanktonic cells. They constitute a major source of dissolved labile organic carbon through lysis or excretion. The reactive organic C can be oxidized by bacterial populations using either oxygen or nitrate as electron acceptor. The rate of the various processes affecting dissolved labile organic carbon is represented in Figure 5(a). At low salinities, there is a high production of labile DOC due to lysis of fresh water phytoplankton which exceeds the removal by respiration. As the redox conditions are not strongly anoxic, the degradation by denitrification remains moderate and small compared to that associated with the utilization of oxygen. Figure 5(b) shows the results given by the model, as well as the observed longitudinal profile of total DOC. The validity of the model calculations is difficult to assess in this case, due to the fact that no direct measurements of the labile DOC are available because of the methodological and conceptual problems.

Phytoplankton

The upper estuary is dominated by large concentrations of fresh water phytoplankton which are rapidly decaying with the increase of salinity. The model predicts that the total respiration of the phytoplankton is almost equal to the gross primary production. The net phytoplankton growth is thus negative and nearly equal to the cell lysis (Figure 6(a)). This situation is due to the fact that primary production is strongly limited by the high turbidity existing in the upper estuary and by the stress induced by the increase of salinity. The decrease of the concentration of carbon associated with the phytoplankton calculated by the model is slower than the measured decrease of chlorophyll. This discrepancy may be partially attributed to the fact that, for the purpose of comparison between model and field data (Figure 6(b)), a constant carbon to chlorophyll ratio (equal to 40 μg C/μg chlorophyll) as been used. It is also interesting to note that the measured phaeopigments profile (an indicator of degraded phytoplanktonic cells) follows the same trend than the calculated phytoplankton curve.

Ammonium

Ammonium is produced by mineralisation of organic matter and consumed by phytoplankton uptake and nitrification. The rates calculated by the model

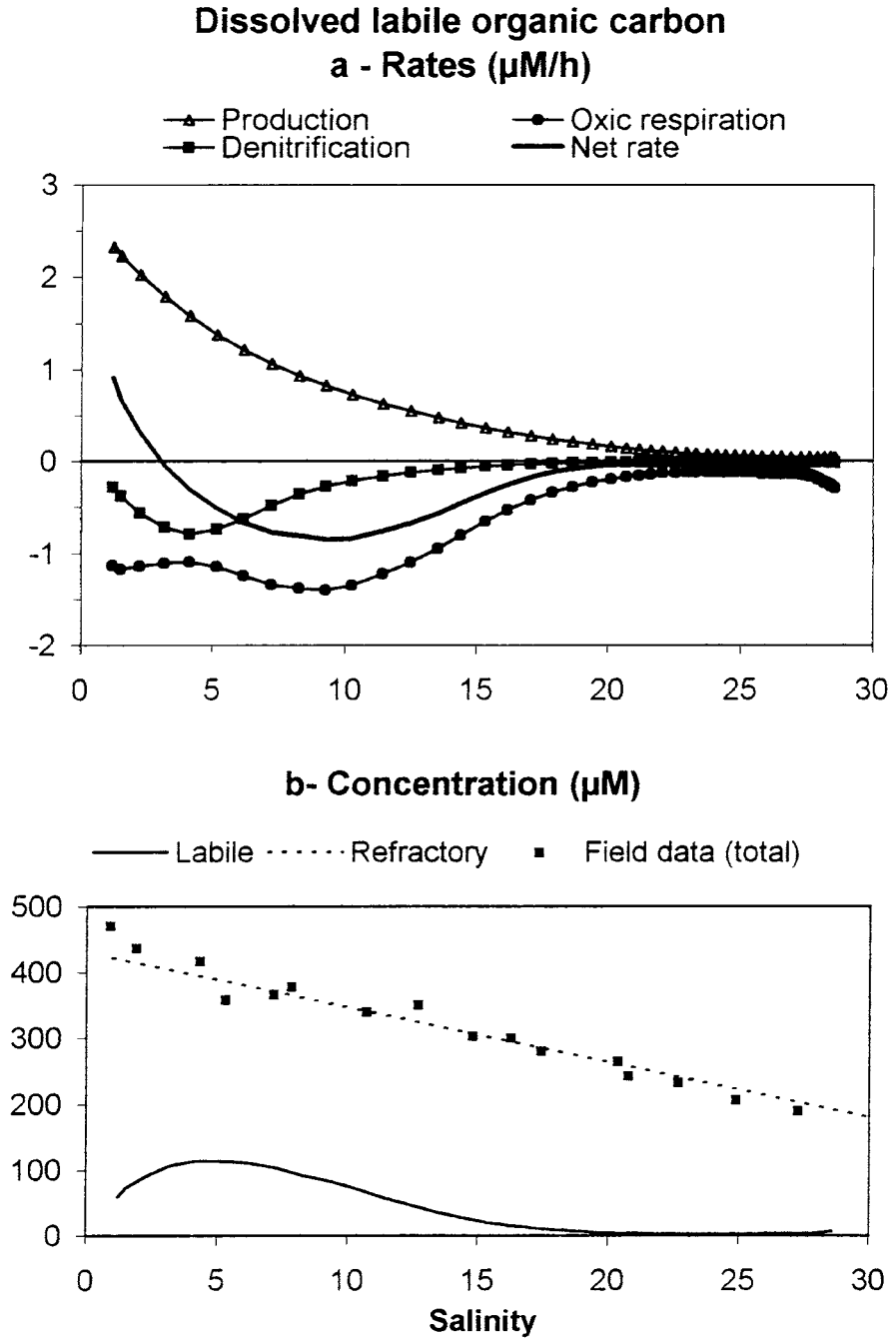

Figure 5. Dissolved labile organic carbon. (a) Longitudinal distribution of the computed process rates. (b) Longitudinal distribution of the computed and measured concentrations.

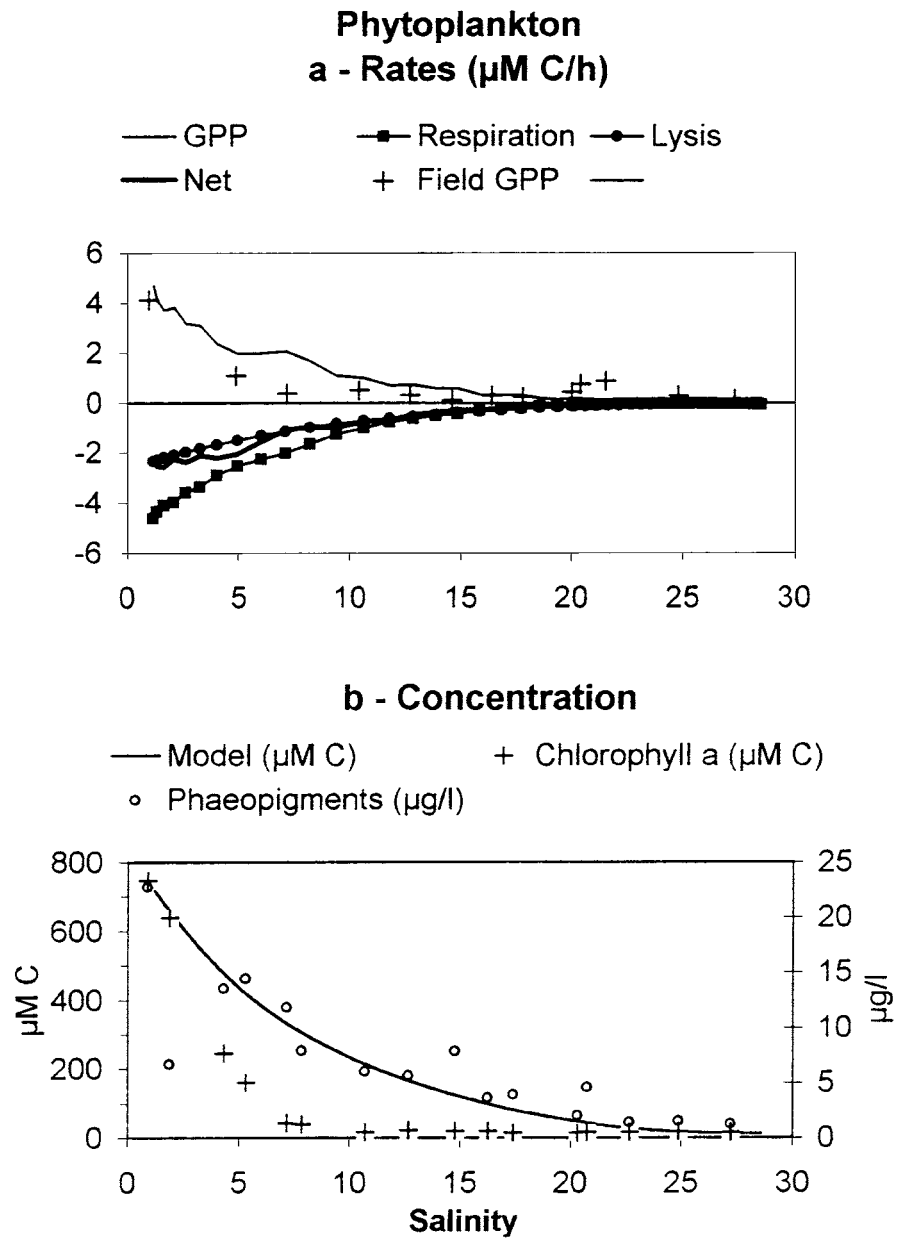

Figure 6. Phytoplankton. (a) Longitudinal distribution of the computed process rates. (b) Longitudinal distribution of the computed and measured concentations.

(Figure 7(a)) show that nitrification is by far the dominant process responsible for the rapid decrease of ammonium concentration in the upper estuary (Figure 7(b)). The model also indicates that the existence of a maximum in nitrification rate around a salinity equal to 3 is due to the optimum development of the nitrifying bacterial biomass at this salinity. It can also be deduced from the model calculation that the concentration of NH_3 in the water column is always very low and remains below the equilibrium value with the atmosphere.

Nitrate

The sub-oxic conditions prevailing in the upper estuary allow for the simultaneous occurrence of nitrification and denitrification (Figure 8(a)). However, the rate of nitrification exceeds largely the rate of denitrification, which explains the maximum concentration of NO_3^- occurring in the estuary (Figure 8(b)). The nitrification curve shown in Figure 8(a) is slightly shifted towards the higher salinities with respect to the consumption curve of ammonium in Figure 7(a). This can be attributed to the accumulation of nitrite as an intermediate product of the nitrification process. Comparison of calculated concentration with field data shows a slight but consistent deviation at mid-salinities. Both the higher computed values and the convexity of the curve are probably due to an overestimation of lateral inputs.

Oxygen

The main processes controlling the concentration of oxygen considered in the model are: aerobic respiration, nitrification, photosynthesis (net primary production) and reaeration (Figure 9(a)). Due to the importance of nitrification in the upper reach, there is a net consumption of oxygen in the region below salinity 8. Oxygen is supplied by exchange with the atmosphere over the whole estuarine length. Photosynthesis may be important locally during daytime (as shown in Figure 9(a) computed for the light conditions at 3 p.m.), but the daily net primary production is always relatively small when the entire estuary is considered. There is a good agreement between calculated and observed profiles of dissolved O_2 (Figure 9(b)). However the calculated values are slightly but systematically lower than the field data in the salinity range 5–15. Here again, the suspected origin of this discrepancy is probably an overestimation of lateral input of detrital organic carbon.

$pH - pCO_2$

In aquatic systems, pH is controlled by the concentration of the dissolved species involved in the buffering capacity of natural waters. In our case, the

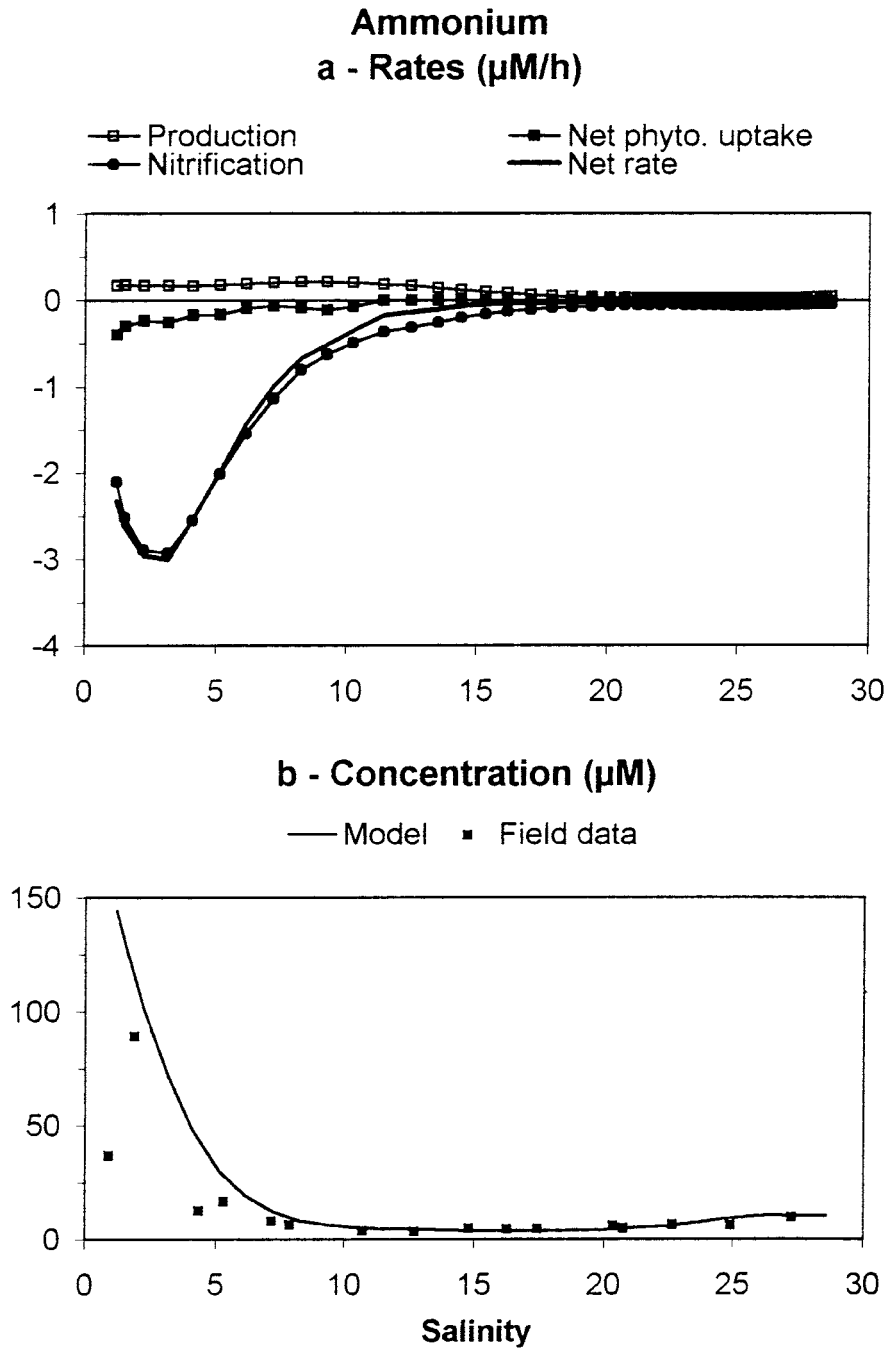

Figure 7. Ammonium. (a) Longitudinal distribution of the computed process rated. (b) Longitudinal distribution of the computed and measured concentrations.

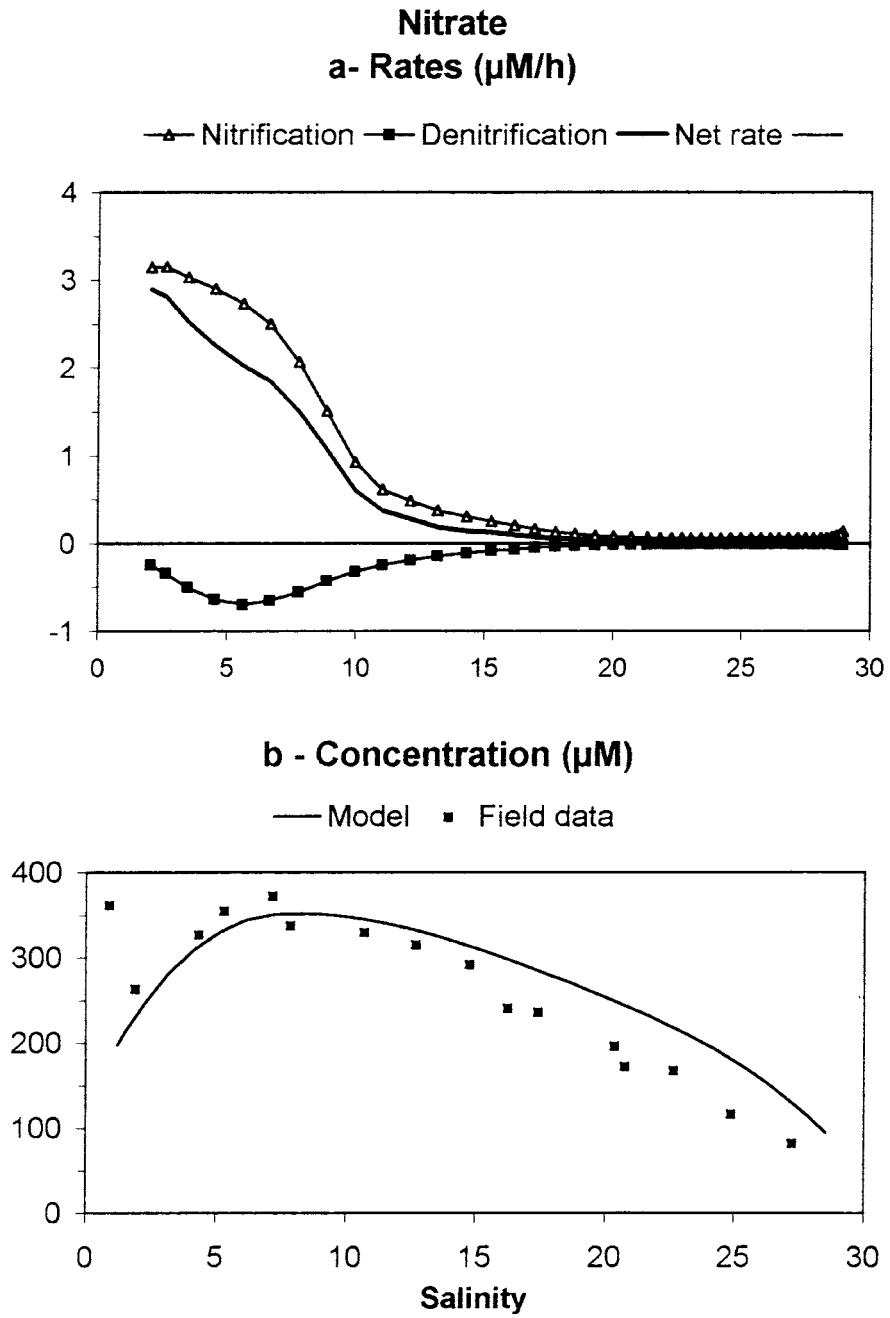

Figure 8. Nitrate. (a) Longitudinal distribution of the computed process rates. (b) Longitudinal distribution of the computed and measured concentrations.

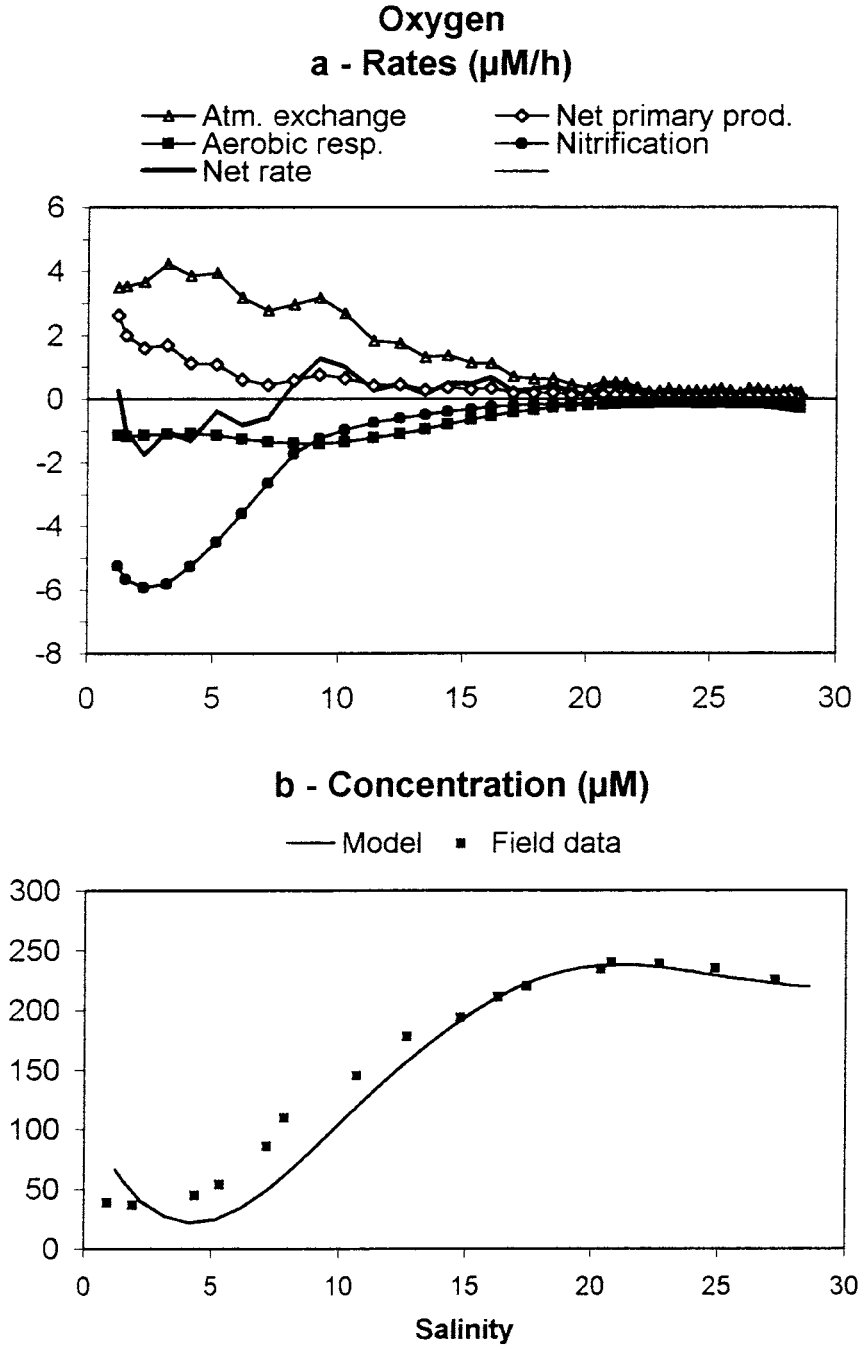

Figure 9. Oxygen. (a) Longitudinal distribution of the computed process rates. (b) Longitudinal distribution of the computed and measured concentrations. Results are given for simulation day 40 at 15h00 (10 July 1996).

pH is essentially controlled by the total concentration of DIC and carbonate alkalinity. Additionally, in the marine part of the estuary, borate species may contribute slightly to the buffer capacity of the system. Both the DIC and the alkalinity are influenced by numerous processes occurring in the estuary. The most important ones considered here are respiration, photosynthesis, nitrification, denitrification and CO_2 exchange with the atmosphere. The calculation of the pH from values of DIC and alkalinity is especially complex in the case of an estuary because of the influence of salinity and temperature on the apparent equilibrium constants. Furthermore, in the vicinity of neutral conditions, pH is very sensitive to small fluctuations of the parameters used in the calculation. Therefore, only a few attempts to model this parameter have been made until now. The knowledge of pH is however crucial when values of pCO_2 are required in order to estimate atmospheric fluxes of this gas. The ability to predict correctly pH may be considered as a severe test for the validation of the model. The results of our calculations are shown in Figure 10. The agreement between calculated and measured values is very satisfactory and better than 0.1 pH unit over the whole estuary. The pH minimum is mainly a consequence of the alkalinity drop due to the nitrification process which releases protons and acidifies the system. Figure 10 also shows that the DIC behaves almost like a conservative component and that the processes other than dilution occurring in the estuary have only a negligible effect on this parameter. The pH changes have however a very marked effect on the pCO_2 values which are largely above the equilibrium with the atmosphere over the entire estuary. The fit of experimental and calculated pCO_2 values is excellent.

Discussion

Carbon dioxide

Using the pCO_2 values presented above and the exchange coefficients at the air-water interface computed by the model, the mean daily fluxes of CO_2 can be calculated (Figure 11). The model shows that the large fluctuation of the CO_2 flux at a fixed upstream location over several tidal cycles (Figure 12) is essentially due to the variation in current velocity and water depth at that point, and is only slightly affected by the tidal oscillation of the water masses. An attempt to evaluate the CO_2 fluxes *in situ* was conducted by continuously recording pCO_2 in the air entrapped in a floating chamber (Frankignoulle 1988). A comparison of the field data with the calculated curve shows that if the general trend of CO_2 atmospheric flux estimated by the two approaches is similar, the calculated values are generally lower than

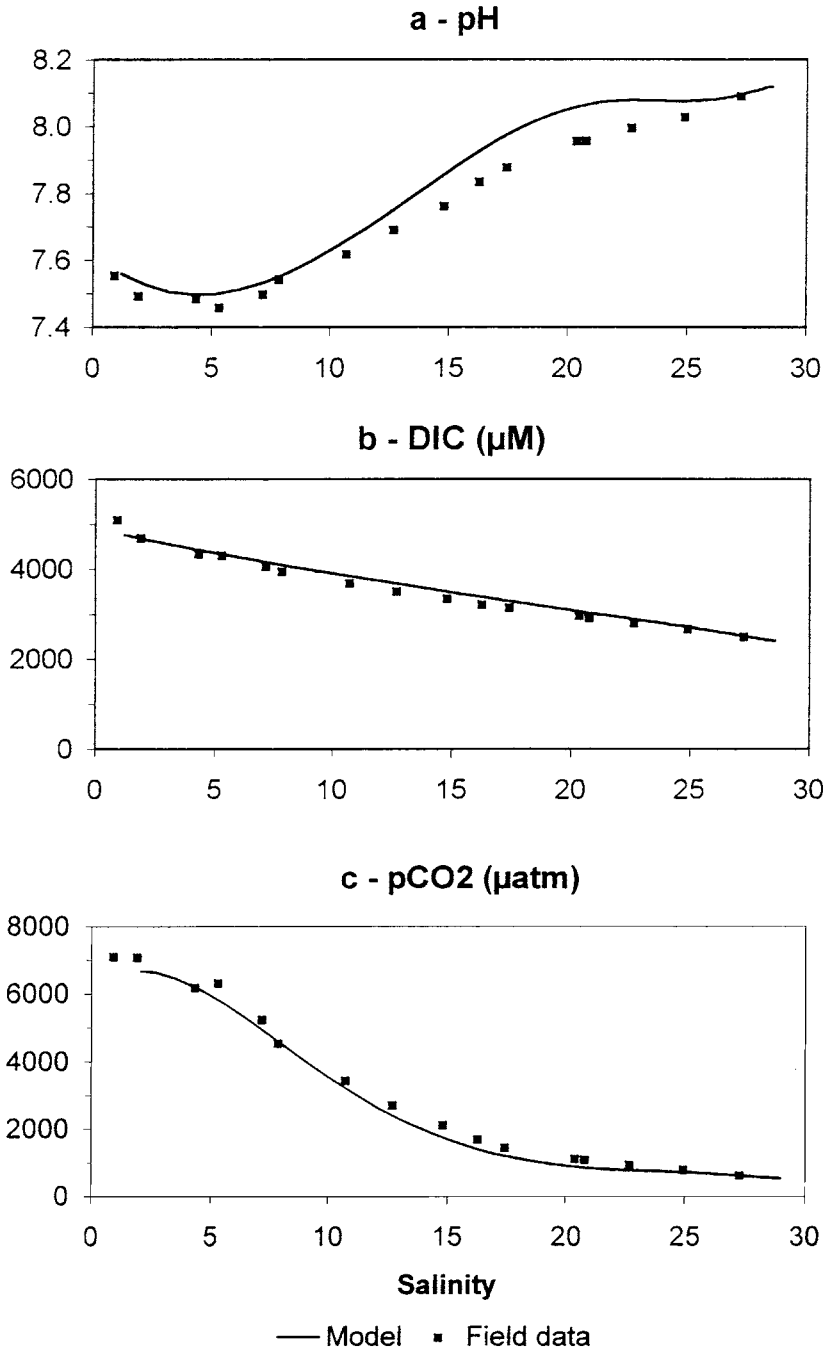

Figure 10. pH and inorganic carbon. (a) Longitudinal distribution of the computed and measured pH. (b) Longitudinal distribution of the computed and measured dissolved inorganic carbon concentration. (c) Longitudinal distribution of the computed and measured CO_2 partial pressure.

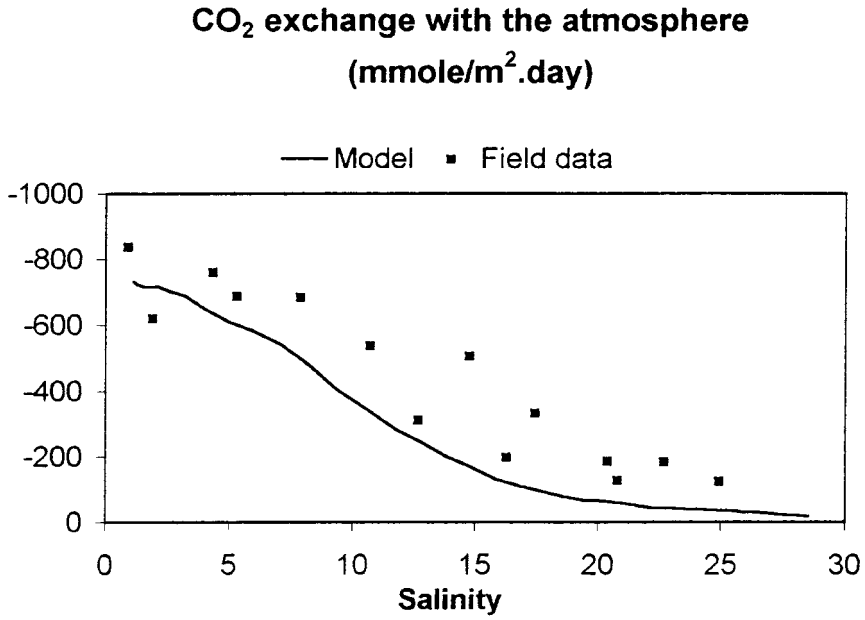

Figure 11. Longitudinal distribution of the computed and measured CO_2 exchange rate per unit surface area.

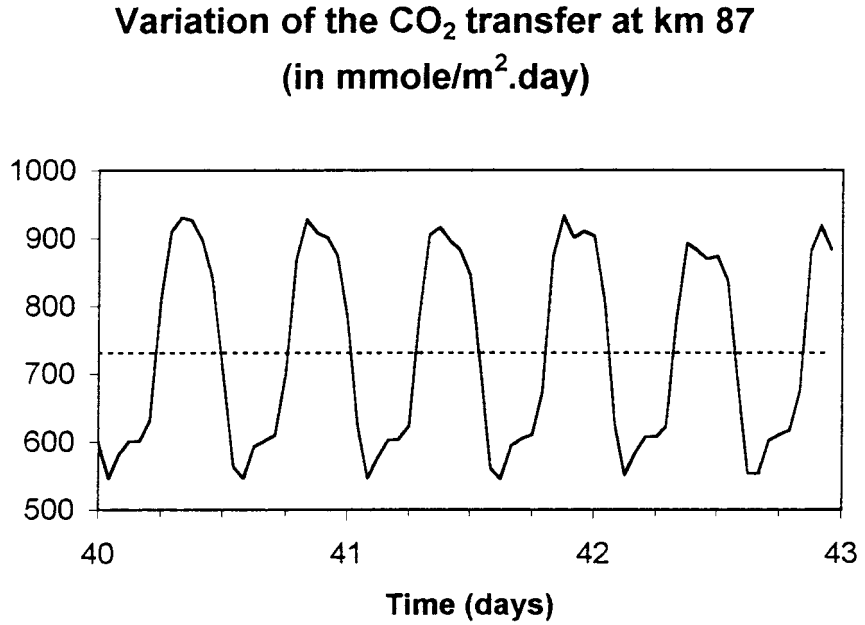

Figure 12. Variation of the computed CO_2 transfer rate (per unit surface area) during 6 tidal cycles at an upstream location (day 40 = 10 July 1996).

the experimental ones. These results could indicate that our model underestimates the exchange coefficients resulting from the combined effects of current and wind speed. We will re-discuss this discrepancy later, on the basis of overall budgets. By taking into account the surface area of the air-water interface, it is also possible to compute the total daily transfer of CO_2 to the atmosphere (Figure 13). In the upper part of this figure we have plotted the tidal average of the surface area for each of the 45-grid cells used in the model as a function of the distance to the sea. The enlargement of the estuarine width leads to a quasi-exponential increase of this surface area. This compensates to a large extent the decrease of the flux (expressed per unit surface area) and as a consequence, each 2-km long grid cell contributes almost equally to the CO_2 transfer. The cumulative CO_2 exchange (Figure 13) follows thus an almost linear pattern. According to these calculations, the daily CO_2 transfer integrated over the entire estuary reaches 225 tons of C per day. Based on the floating chamber approach, the total CO_2 transfer estimated by Frankignoulle et al. (1998) for the same period is equal to 550 T C day^{-1}. The large discrepancy between the two estimates mainly originates from the higher CO_2 fluxes obtained by Frankignoulle et al. (1998) in the high salinity range, which also corresponds to the largest air-water interface areas.

Oxygen

To elucidate the origin of the difference in the CO_2 flux estimations, we have performed mass balance calculations for oxygen which is closely related to carbon but offers the advantage of having a much simpler speciation than the inorganic carbon system. The mass balance is obtained by integrating the fluxes at the boundaries (river, sea, atmosphere) and the rates of the processes affecting oxygen (aerobic respiration, nitrification, exchange with the atmosphere) over one tidal cycle. The results of these model calculations are presented in Figure 14. The total oxygen input (33.3×10^6 moles.day^{-1}) is nearly balanced by the total output (36.1×10^6 moles.day^{-1}), indicating that the system is not far from steady state conditions. The consumption of oxygen respectively by respiration and by nitrification are nearly equal, and the sum is balanced by the reaeration process. Other contributions are marginal. It is interesting to note that the CO_2 transfer calculated above (225 tons C day^{-1} = 19×10^6 moles C day^{-1}) is in close agreement with the respiration term calculated in the oxygen budget. The only possibility to obtain a better agreement between the CO_2 flux calculated by the model and that estimated from *in situ* measurements by Frankignoulle et al. (1998) (550 tons C day^{-1} = 46×10^6 moles C day^{-1}) would be to considerably increase both the respiration flux and the gas exchange coefficient. Simulations have been made accordingly, but the resulting longitudinal profiles are far from

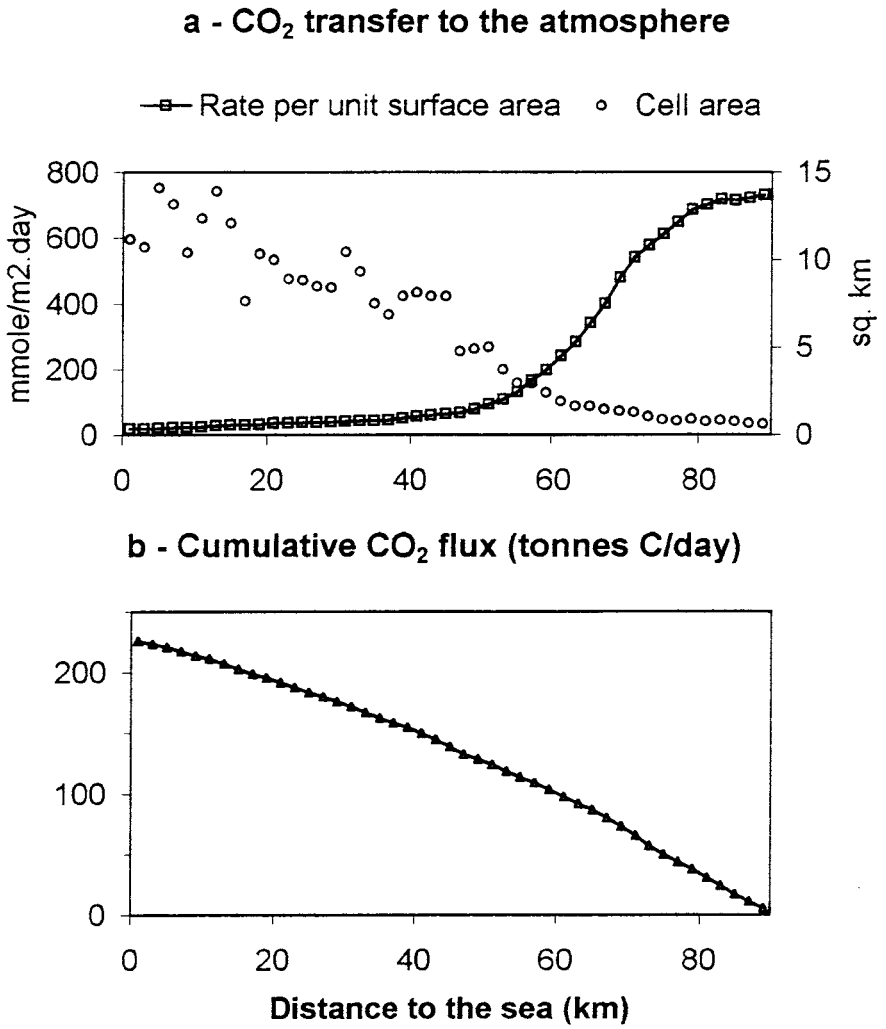

Figure 13. Total computed daily flux of CO_2 to the atmosphere. (a) Longitudinal distribution of the CO_2 exchange rate per unit area; longitudinal evolution of the estuarine surface area. Cell area refers to the 45 grid cells of the model. (b) Cumulative CO_2 flux (summation starting upstream).

the field observations, not only for oxygen but also for pH and nitrogen species. Furthermore, a doubling of the piston velocities of the biogases seems excessive and unlikely. The overall consistency of the model results imposes a limited range of CO_2 production and emission to the atmosphere.

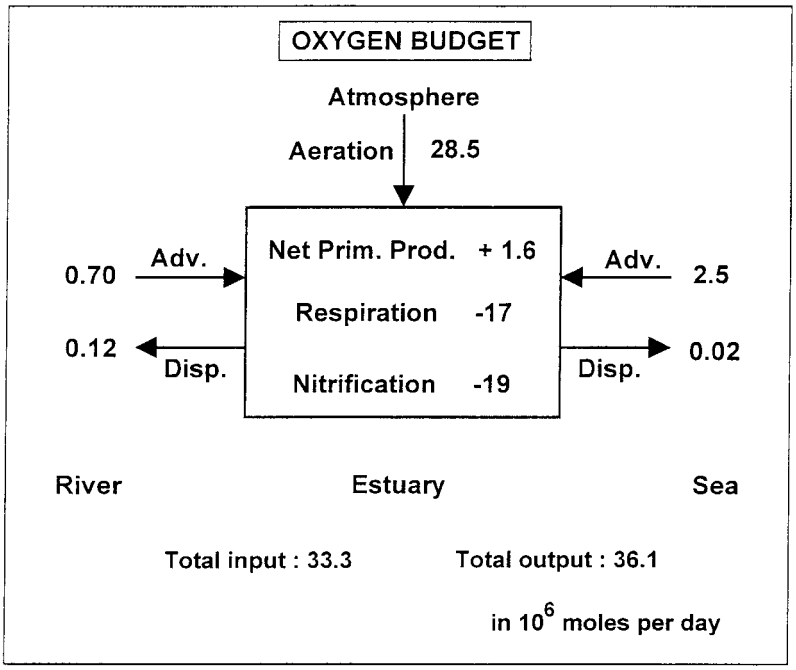

Figure 14. Daily mass balance of oxygen over the estuarine zone (computed *by the model* for July 10th, 1996). ADV = advective flux, DISP = dispersive flux.

Nitrogen oxide and ammonia

The model allows estimation of the production of N_2O associated with the intense nitrification process occurring in the upper estuary. The concentration profile (Figure 15(a)) resulting from the combined effect of biological production and degassing to the atmosphere shows a slightly lower maximum which is shifted seaward with respect to the measured values. This is probably due to the fact that the N_2O yield is taken here as constant although it is known that it may vary by one order of magnitude, increasing at low O_2 concentrations (De Wilde & De Bie 2000). Also, denitrification occurring in the sub-oxic zone could contribute to some N_2O production, but this process is presently not implemented in the model. Similarly to CO_2, the N_2O flux exhibits very high values upstream (Figure 15(b)), while the total transfer is distributed more homogeneously along the estuary due to the increasing surface area seawards (Figure 15(c)). The integrated transfer over the entire estuary reaches 17 kmoles.day^{-1}, which is in good agreement with the value proposed by De Wilde and De Bie (2000) equal to 13.9 kmoles·day^{-1} for this period, based on their own measurements and calculations. As indicated earlier, the pH values are low enough to prevent high concentrations

of ammonia in the Scheldt. This gas remains always undersaturated with respect to the atmosphere and there is thus a very small flux of NH_3 from the atmosphere to the water column.

Conclusions

CONTRASTE is the first attempt to include the emissions of biogases other than oxygen in estuarine models, and to provide a dynamical pH simulation for this type of environment. In the case of CO_2, this imposes a detailed description of the various processes affecting the carbon cycle and the physico-chemical properties of the inorganic carbon system. The degree of saturation of CO_2 with respect to the atmosphere is very sensitive to the pH and, therefore, this parameter must be carefully estimated. In the case of the Scheldt, the pH is strongly affected by the nitrification process which modifies the alkalinity of the system. Due to the fact that we consider a large number of parameters which are closely interrelated in various processes, severe constraints are imposed on the values of the model parameters. The overall agreement obtained between observed and computed profiles in the estuary is thus a reliable indication of the model validity.

The experimental evaluation of biogas fluxes to the atmosphere in tidal estuaries is particularly difficult because of short- and long-term fluctuations of the physical forcing. There are in addition serious methodological problems associated with direct flux measurements. For the short period of time for which intensive field data were available (July 1996), a good agreement was obtained between the calculated and observed values of the partial pressure of O_2, CO_2 and N_2O. In the case of the CO_2 flux to the atmosphere, there was however discrepancies by a factor of two between the model calculations and estimations based on *in situ* point measurements. Our confidence in the model results is however supported by the consistency between the carbon and oxygen budget. We suspect a small but systematic overestimation in the measured CO_2 fluxes with the experimental device used. This may have a large effect in the lower part of the estuary where the exchange per unit surface area is small but where the exchange surface area is very large. Nevertheless, our estimations of the fluxes of CO_2 and N_2O in the Scheldt estuary confirm that this highly disturbed system is responsible for a very high release of these biogases to the atmosphere. These results strongly support the use of transient reactive-transport models for the estimation of time and space integrated fluxes. It also highlights the importance of *in situ* rate measurements for model validation. However, greater emphasis should be given in the future towards a more integrated approach between the design of field experiments and the model build-up.

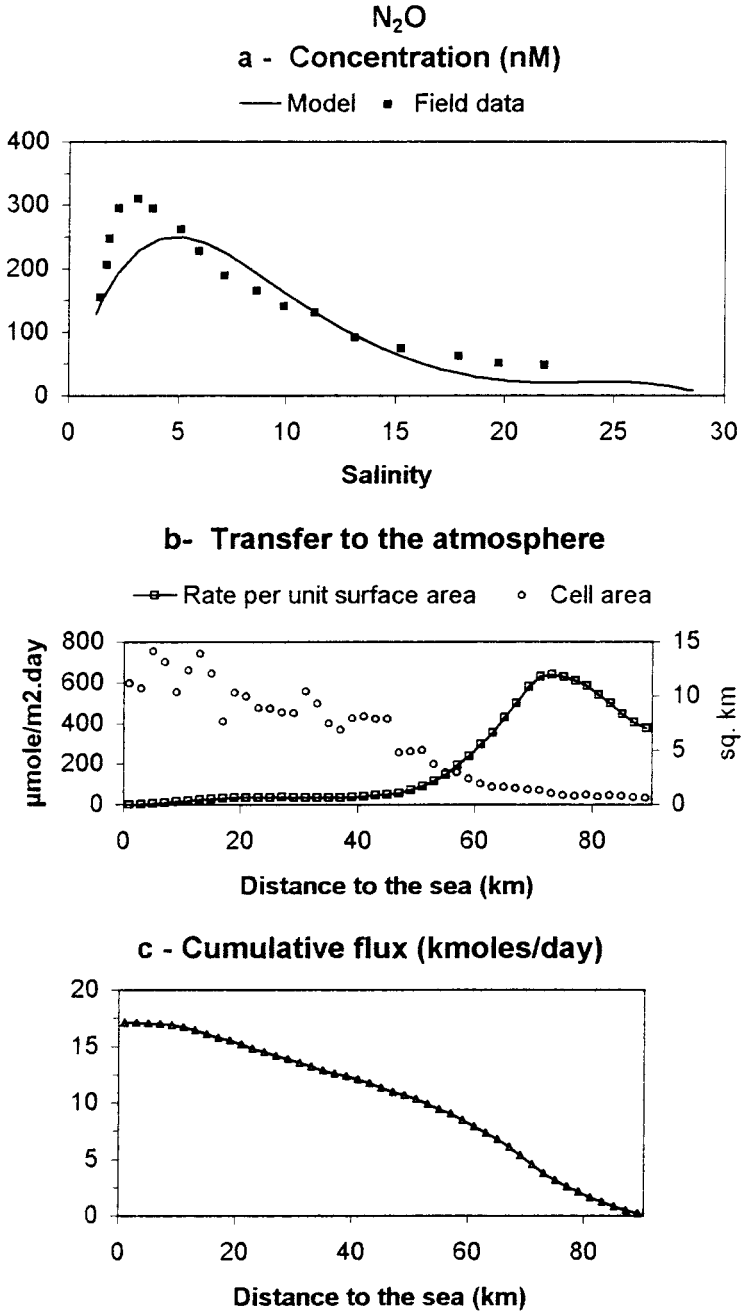

Figure 15. Nitrogen oxide. (a) Longitudinal distribution of the computed and measured N_2O concentrations. (b) Longitudinal distribution of the N_2O exchange rate per unit area; longitudinal evolution of the estuarine surface area. (c) Cumulative N_2O flux (summation starting upstream).

Acknowledgements

We thank D. Bajura, N. Canu, L. Chou, S. De Beer, K.T. Dotansi and V. Herzl for their cooperation in analytical and logistic support. The close collaboration of our colleagues from all teams involved in the BIOGEST project is greatly appreciated with special acknowledgement to the project coordinator M. Frankignoulle. The authors also like to thank J. Backers of the *Management Unit of the North Sea Mathematical Models* (Belgium) for providing CTD and meteorological data, the officers and the crew of *R.V. Belgica* for their cooperation during the July 1996 field campaign and the *Ministerie van de Vlaamse Gemeenshap, Departement Leefmilieu en Infrastructuur, Afdeling Maritieme Schelde* (Belgium) for supplying discharge data of the Scheldt. This work was funded by the European Commission (BIOGEST project no. ENV4-CT96-0213). This is an Eloise contribution no. 229.

References

Benson BB & Krause D (1984) The concentration and isotopic fractionation of oxygen dissolved in freshwater and seawater in equilibrium with the atmosphere. Limnol. Oceanogr. 23: 620–632

Billen G, Lancelot C, De Becker E. & Servais P (1988) Modelling microbial processes (phyto- and bacterioplankton) in the Scheldt estuary. Hydrobiol. Bull. 22: 43–55

Brion N & Billen G (1998) A re-assessment of $H^{14}CO_3^-$ incorporation method for measuring autotrophic nitrification and its use to estimate nitrifying biomasses. Revue des Sciences de l'Eau 11: 283–302

Cai W & Wang Y (1998) The chemistry, fluxes, and sources of carbon dioxide in the estuarine waters of the Satilla and Altamaha Rivers, Georgia. Limnol. Oceanog. 43: 657–668

Clegg S & Whitfield M (1995) A chemical model of seawater including dissolved ammonia and stoichiometric dissociation constant of ammonia in estuarine water and seawater from –2 to 40 °C. Geochim. Cosmochim. Acta 59: 2403–2421

De Wilde HPJ & de Bie MJM (2000) Nitrous oxide in the Schelde estuary: production by nitrification and emission to the atmosphere. Mar. Chem. 69: 203–216

Dronkers J (1964) Tidal Composition in Rivers and Coastal Waters. North-Holland, New-York

Edmund JM & Gieskes JM (1970) On the calculation of degree of saturation of seawater with respect to calcium carbonate under *in situ* conditions. Geochim. Cosmochim. Acta 34: 1261–1291

Frankignoulle M (1988) Field measurements of air-sea CO_2 exchange. Limnol. Oceanogr. 33: 313–322

Frankignoulle M, Bourge I & Wollast R (1996) Atmospheric CO_2 fluxes in a highly polluted esturay (the Scheldt). Limnol. Oceanoghr. 41: 365–369

Frankignoulle M, Abril G, Borges A, Bourge I, Canon C, Delille B, Libert E & Theate JM (1998) Carbon dioxide emission from European estuaries. Science, 282: 434–436

IRM (1996) Bulletin mensuel de l'Institut Royal Météorologique de Belgique. Observations climatologiques, Partie I et II, Juin–Juillet 1996. In: Malcorps H (Ed) Bruxelles. 39 + 36 pp

Mehrbach C, Cuberson CH, Hawley JE & Pytkowicz RM (1973) Measurement of the apparent dissociation constants of carbonic acid in seawater at atmospheric pressure. Limnol. Oceanogr. 18: 897–907

Mook WG & Koene BKS (1975) Chemistry of dissolved inorganic carbon in estuarine and coastal brackish waters. Estuar. Coastal Mar. Sci. 3: 325–336

O'Connor DJ & Dobbins WE (1956) Mechanism of reaeration in natural streams. J. Sanitary Eng. Div. ASCE 82(SA6): 1–30

Platt T, Gallegos CL & Harisson WG (1980) Photoinhibition of photosynthesis in natural assemblages in marine phytoplankton. J. Mar. Res. 38: 687–701

Platt T, Satthyendranath S & Ravindran P (1990) Primary production by phytoplankton: analytic solutions for daily rates per unit area of water surface. Proc. R. Soc. Lond. 241: 101–111

Regnier P, Wollast R & Steefel CI (1997) Long term fluxes of reactive species in macrotidal estuaries: Estimates from a fully transient, multi-component reaction transport model. Mar. Chem. 58: 127–145

Regnier P, Mouchet A, Wollast R & Ronday F (1998) A discussion of methods for estimating residual fluxes in strong tidal estuaries. Cont. Shelf Res. 18: 1543–1571

Regnier P & Steefel CI (1999) A high resolution estimate of the inorganic nitrogen flux from the Scheldt estuary to the coastal North Sea during a nitrogen-limited algal bloom, Spring 1995. Geochim. Cosmochim. Acta 63: 1359–1374

Sander R (1999) Compilation of Henry's law constants for inorganic and organic species of potential importance in environmental chemistry. http://www.mpch-mainz.mpg.de/~sanders/res /henry.html

SAWES (1991) Waterkwaliteitsmodel Westerschelde. WL-rapport T527.

Soetaert K & Herman PMJ (1993) MOSES-model of the Scheldt estuary: Ecosystem model development under SENECA. Report NIOO. Yerseke, The Netherlands

Somville M (1984) Use of nitrifying activity measurements for describing the effect of salinity on nitrification in the Scheldt estuary. Appl. Environ. Microbiol. 47: 424–426

Van Damme S, Meire P, Maeckelberghe H, Verdievel M, Bourgoing L, Taveniers E, Ysebaert T & Wattel G (1995) De waterkwaliteit van de zeeschelde: evolutie in de voorbije dertig jaar. Water 85: 244–256. In Dutch with a summary in English

Wanninkhof R (1992) Relationship between wind speed and gas exchange over the ocean. J. Geophys. Res. 97: 7373–7382

Weiss RF & Price BA (1980). Nitrous oxide solubility in water and seawater. Mar. Chem. 8: 347–359

Wollast R (1988) The Scheldt estuary. In: Salomon W, Bayne B, Duursma EK & Forstner U (Eds) Pollution of the North-Sea: An Assessment (pp 183–193). Springer Verlag